New Mexico Geological Society

Downloaded from: https://nmgs.nmt.edu/publications/guidebooks/46



$^{40}Ar/^{39}Ar$ geochronology of tephra layers in the Santa Fe Group, Espanola Basin, New Mexico

William C. McIntosh and Jay Quade
1995, pp. 279-287. https://doi.org/10.56577/FFC-46.279

in:

Geology of the Santa Fe Region, Bauer, P. W.; Kues, B. S.; Dunbar, N. W.; Karlstrom, K. E.; Harrison, B.; [eds.], New Mexico Geological Society 46 th Annual Fall Field Conference Guidebook, 338 p. https://doi.org/10.56577/FFC-46

This is one of many related papers that were included in the 1995 NMGS Fall Field Conference Guidebook.

Annual NMGS Fall Field Conference Guidebooks

Every fall since 1950, the New Mexico Geological Society (NMGS) has held an annual Fall Field Conference that explores some region of New Mexico (or surrounding states). Always well attended, these conferences provide a guidebook to participants. Besides detailed road logs, the guidebooks contain many well written, edited, and peer-reviewed geoscience papers. These books have set the national standard for geologic guidebooks and are an essential geologic reference for anyone working in or around New Mexico.

Free Downloads

NMGS has decided to make peer-reviewed papers from our Fall Field Conference guidebooks available for free download. This is in keeping with our mission of promoting interest, research, and cooperation regarding geology in New Mexico. However, guidebook sales represent a significant proportion of our operating budget. Therefore, only *research papers* are available for download. *Road logs*, *mini-papers*, and other selected content are available only in print for recent guidebooks.

Copyright Information

Publications of the New Mexico Geological Society, printed and electronic, are protected by the copyright laws of the United States. No material from the NMGS website, or printed and electronic publications, may be reprinted or redistributed without NMGS permission. Contact us for permission to reprint portions of any of our publications.

One printed copy of any materials from the NMGS website or our print and electronic publications may be made for individual use without our permission. Teachers and students may make unlimited copies for educational use. Any other use of these materials requires explicit permission.

This page is intentionally left blank to maintain order of facing pages.

$^{40}AR/^{39}AR$ GEOCHRONOLOGY OF TEPHRA LAYERS IN THE SANTA FE GROUP, ESPAÑOLA BASIN, NEW MEXICO

WILLIAM C. McINTOSH[1] and JAY QUADE[2]

[1]New Mexico Bureau of Mines and Mineral Resources, New Mexico Institute of Mining and Technology, Socorro, NM 87801; [2]Department of Geosciences/Desert Laboratory, University of Arizona, Tucson, AZ, 85721

Abstract—Laser-fusion $^{40}Ar/^{39}Ar$ analyses yield high-precision, stratigraphically consistent ages for a sequence of tephra layers within Santa Fe Group strata in the Española Basin, northern New Mexico. Ages determined for crystals from individual tephra layers are tightly grouped within samples and agree closely with stratigraphic order:

Formation	*Member*	*Tephra*	*Mineral*	*Age(Ma)*
Chamita Fm	upper tuffaceous member	upper ashes	sanidine	6.78 ±0.03
Chamita Fm	upper tuffaceous member	lower ash	sanidine	6.93 ±0.05
Chamita Fm	lower tuffaceous member	lower ash	hornblende	7.7 ±0.3
Tesuque Fm	Skull Ridge Member	White Ash #4	sanidine	15.45 ±0.06

These $^{40}Ar/^{39}Ar$ results help refine age estimates of the Tesuque and Chamita Formations, which have been subjects of previous controversy. The 15.45 Ma age for White Ash #4 confirms the general scheme of paleomagnetic correlations for the Skull Ridge Member proposed by Barghoorn (1981) and Tedford and Barghoorn (1993), but contradicts previous younger zircon fission-track ages. Early Barstovian fossils found in the White Operation Quarry just below White Ash #4 date to ~15.4 Ma. The results from the lower (7.7 Ma) and upper (6.95-6.75 Ma) tuffaceous zones of the Chamita Formation conflict with previous interpretations of Chamita Formation age based on magnetostratigraphy and too-young fission track dates (5.3 and 5.6 Ma). However, a recalibration of magnetostratigraphy with $^{40}Ar/^{39}Ar$ results matches well with recent revisions of the geomagnetic polarity time scale (Cande and Kent, 1992). The important late Hemphillian fossils found in the San Juan and Rak quarries in the upper tuffaceous zone are now dated to between 6.95 and 6.75 Ma. Based on the age and K/Ca ratios of sanidine, tephra layers in the upper tuffaceous zone represent distal fall facies of the Peralta Tuff, a rhyolite-dome-related pyroclastic sequence erupted 40-50 km to the southwest.

INTRODUCTION

The Santa Fe Group in the Española Basin contains important records of Neogene climate, biostratigraphy, mammalian evolution, and tectonic development of the northern Rio Grande rift. Infilling of this segment of the rift began in the Oligocene and continues today (Ingersoll et al., 1990). The Santa Fe Group, conspicuously exposed throughout the Española Basin, represents much of the Neogene portion of the rift-filling history. Early interest in the Santa Fe Group centered on mammalian fossil remains collected from throughout the section, and the paleontological richness of the deposits continues to attract research (Galusha and Blick, 1971; MacFadden, 1976, 1977; Tedford and Barghoorn, 1993). The importance of the Santa Fe Group to understanding the tectonic and sedimentary development the rift has also received much attention (e.g., Cavazza, 1986,1989; Ingersoll et al., 1990; Cather, 1992).

The Tesuque and Chamita Formations of the Santa Fe Group in the Española Basin (Fig. 1) contain numerous, laterally persistent tephra layers, which have been mapped and used as stratigraphic markers by several workers (e.g., Galusha and Blick, 1971; Tedford and Barghoorn, 1993; Rhoads and Smith, this volume). Tephra layers in the Tesuque Formation are generally very fine grained (silt-sized), 10 cm to 3 m thick, and are distributed through much of the unit (Fig. 2). Tephra layers in the Chamita Formation (Fig. 2) are typically coarser than those in the underlying Tesuque Formation, and are generally restricted to two 50-m-thick intervals termed the lower tuffaceous zone and upper tuffaceous zone by MacFadden (1976, 1977). Considerable age control for the Tesuque and Chamita Formations has been provided by fossils (summarized by Tedford and Barghoorn, 1993), magnetostratigraphy (MacFadden, 1976, 1977; Barghoorn, 1981), and limited fission-track dating of the tephras (Manley and Naeser, 1977; Izett and Naeser, 1986).

In this study we employed high-precision, single-crystal $^{40}Ar/^{39}Ar$ methods to date tephra layers in the Tesuque and Chamita Formations, thereby testing and refining previously proposed chronologies. Developing a precise, reliable chronology for the Española Basin is critical to studies that use the basin-fill sequence for reconstructions of Neogene climate, biological or tectonic history. In addition to dating tephra layers, we also used single-crystal $^{40}Ar/^{39}Ar$ methods to redate samples of

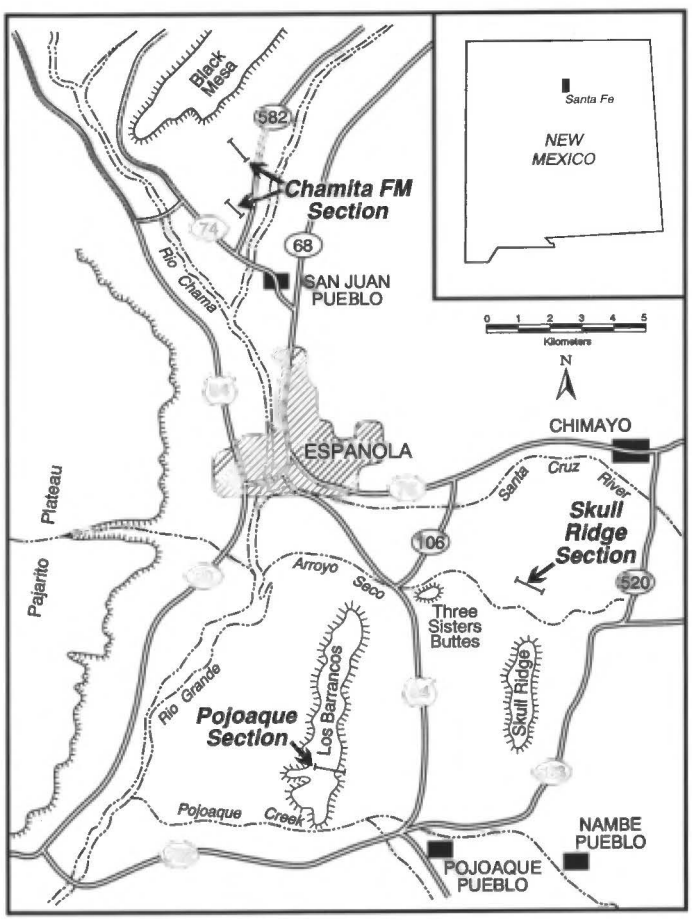


FIGURE 1. Map of study area showing sample locations.

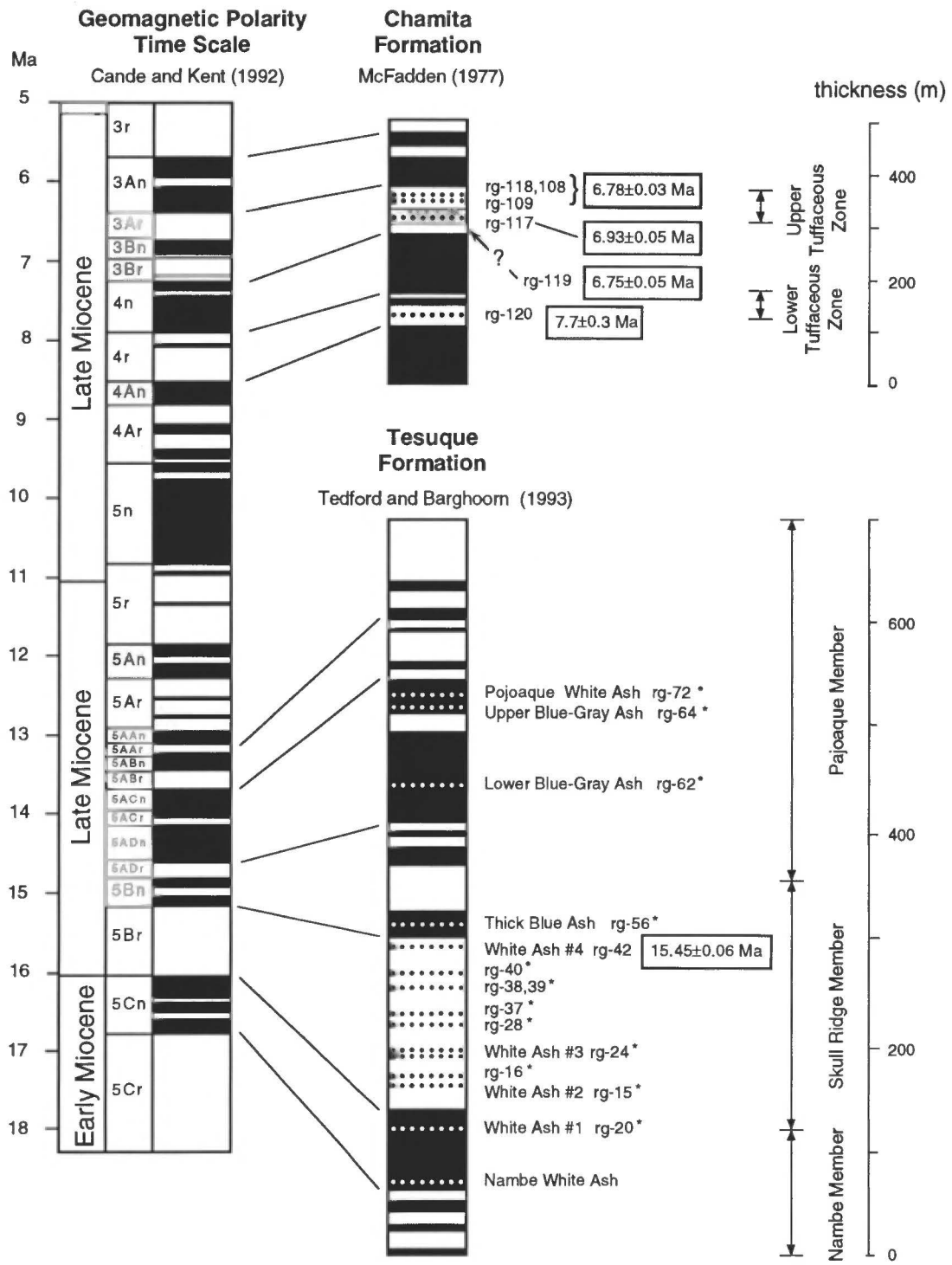


FIGURE 2. Measured stratigraphic sections showing named tephra layers, stratigraphic distribution of samples, and magnetostratigraphy of Tesuque and Chamita Formations. Black denotes normal polarity and white denotes reversed polarity. Starred samples were not successfully dated.

the Peralta Tuff, a dome-related pyroclastic sequence exposed in the southeastern Jemez Mountains. These analyses were done because published age determinations from the Peralta Tuff (McIntosh and Harlan, 1991) suggested possible correlations with tephra layers in the upper tuffaceous zone of the Chamita Formation.

MEASURED SECTIONS

The exhaustive study of Galusha and Blick (1971) provides a logical framework for continuing studies of Santa Fe Group stratigraphy. We measured sections in the same areas as their study, and attempted to relocate all key marker tephras. We adhere to Galusha and Blick's nomenclature of the tephras throughout most of this text.

Our measured section for the Tesuque Formation parallels Arroyo Seco on the north side, about 1.5 km NW of NM-503 connecting Nambe Pueblo and Rancho de Chimayo (Fig. 1). The measured section lies entirely in Section 15, T20N, R9E (Cundiyo 7.5'), where Galusha and Blick (1971) measured their sections. Many landmarks and major tephras described by Galusha and Blick were relocated. We started measurement at White Ash #1, conspicuously exposed at the base of the "Red Wall" north of Arroyo Seco (Galusha and Blick, 1971, fig. 15B), and terminated the

section at White Ash #4. Our measured stratigraphic thicknesses in the Skull Ridge Member closely match the thicknesses given by Galusha and Blick, and we felt secure in identifying White Ash #1, 2, F and 4. However, the exact trace of the Galusha and Blick section was not published, and our traverse is probably not identical to theirs. The section contains numerous lesser tephras, which in many cases thin or disappear laterally. We sampled many of these lesser tephras but, given their lateral variability, did not attempt to identify them with those numbered by Galusha and Blick. We measured the Pojoaque Member of Tesuque Formation starting at the base of Los Barrancos and carried over the ridge until the section is repeated by faulting, in the same area measured by Galusha and Blick (1971). Our section lies entirely within the S½ sec. 15, T20N, R8E, starts just below the Lower Blue-Gray Ash, and ends about 150 m above the Pojoaque White Ash. These tephras and the Upper Blue-Gray Ash stand out, and our stratigraphic thicknesses between these marker beds closely match those of Galusha and Blick. Several small normal faults cut the section in this traverse, and particular care was taken to not repeat portions of measured sections.

The Chamita Formation stratotype is exposed below Black Mesa on the San Juan Pueblo Reservation. Both Galusha and Blick (1971), and MacFadden (1976, 1977) measured sections in this area, and collected samples for dating. We did not produce a detailed stratigraphic log for the Chamita Formation, and confined our sampling to the two major tuffaceous zones, which we relocated using Galusha and Blick's descriptions and field notes kindly supplied by B. MacFadden. We sampled tephras in the tuffaceous zones at several localities (Fig. 2). The upper tuffaceous zone is well exposed over a large area, and all our samples come from just south of Arroyo Los Borregos. The lower tuffaceous zone is less conspicuous and is also offset by faults of unknown displacement in our sampling area (NW1/4 sec. 10, T21N, R8E). As we discuss later, this complexity introduces some problems in interpreting the $^{40}Ar/^{39}Ar$ results from there, which will only be resolved with detailed mapping.

METHODS

From the measured sections detailed above, 25 samples were collected for $^{40}Ar/^{39}Ar$ analysis (Fig. 1). Our goal in the field was to obtain tephra samples as free from detrital contamination as possible, so many tephras were scrutinized laterally and vertically for the cleanest material. Some tephra layers were sampled at multiple localities. Samples were typically 1-5 kg of unlithified to slightly lithified tephra. Sanidine or hornblende separates were prepared from tephra samples by crushing and sieving samples to 50-800 μm, ultrasonically cleaning them in dilute (7%) hydrofluoric acid, then applying magnetic and density-liquid techniques, followed by hand picking. For some tephra layers entirely lacking phenocrysts, separates of glass shards were prepared by similar methods. In addition to samples from the Tesuque and Chamita Formations, new sanidine separates were prepared from five samples of Peralta Tuff and a related lava that were previously dated by $^{40}Ar/^{39}Ar$ bulk-sample, step-heating methods at 7.08 to 6.71 Ma (McIntosh and Harlan, 1991). Aliquots (10-20 mg) of each mineral and glass separate were packaged with alternating flux monitors of Fish Canyon Tuff sanidine (27.84 Ma, relative to MMhb-1 hornblende at 520.4 Ma; Samson and Alexander, 1987) and irradiated in the L67 position of the Ford reactor at the University of Michigan.

$^{40}Ar/^{39}Ar$ analyses were performed at the New Mexico Geochronology Research Laboratory at the New Mexico Institute of Mining and Technology. This facility includes an MAP 215-50 mass spectrometer attached to a fully-automated all-metal argon extraction system equipped with a 10 watt CO_2 laser. Crystals from sanidine-bearing samples of the Peralta Tuff and the upper tuffaceous zone of the Chamita Formation were large enough to allow laser-fusion analysis of single grains. Typically, 8 to 12 grains from each of these samples were individually analyzed. For samples where crystals or glass shards were too small for single-grain analyses, 8 to 12 different groups of 10 to 40 grains were fused and analyzed. Samples analyzed by this multiple crystal approach include hornblende from a tephra in the lower tuffaceous zone of the Chamita Formation and sanidine and glass from tephra layers within the Pojoaque and Skull Ridge Members of the Tesuque Formation. Samples and monitors were fused by CO_2 laser for 15 seconds, then reactive gasses were removed using a SAES GP-50 getter prior to expansion into the mass spectrometer. Extraction line blanks during these analyses ranged from 5×10^{17} to 2×10^{16} moles ^{40}Ar and 5×10^{19} to 2×10^{18} moles ^{36}Ar. The neutron flux values (J-values) within irradiation packages were determined to a precision of ±0.25% by averaging results of four subsamples (each 1-4 crystals, approximately 1 mg) of each sanidine monitor.

RESULTS

Precise ages were obtained from 12 of the 24 samples (Table 1; Appendix). The successful age determinations include 10 single-crystal analyses, of coarse sanidine from samples of the Peralta Tuff and the upper tuffaceous zone of the Chamita Formation, plus two multiple crystal analyses one of hornblende from the lower tuffaceous zone of the Chamita Formation sample and one of fine sanidine from White Ash # 4 from the Skull Ridge Member, Tesuque Formation. As described below, analyses of 12 other fine-grained K-feldspar or glass shards yielded inconsistent or geologically unreasonable ages.

For the 10 samples of coarse (0.2-0.8 mm) sanidine, single-crystal laser-fusion analyses produced precise ages for individual crystals, with 1s analytical precision typically from ±0.25 to ±0.5%. Radiogenic yields were generally high (95-100%) and K/Ca values typically ranged from 35 to 60. Within the population of grains from each sample, single-crystal ages and K/Ca values were tightly grouped (Figs. 3, 4; Appendix). Mean ages, K/Ca values, and 1s errors were calculated for each sample from the individual crystal data (Table 1) after excluding a small number of aberrant analyses (open circles in Figs. 3, 4). Mean ages for these ten

TABLE 1. Summary of $^{40}Ar/^{39}Ar$ results from Española Basin tephras and Peralta Canyon tuffs.

Sample	Unit	L#	min	n	Age	Error	K/Ca	Error
Santa Fe Group tephras, Espanola Basin								
RG-118	Chamita Fm, upper tuffaceous zone, 354 m	1678	san	7	6.79	0.02	45.1	4.0
RG-108	Chamita Fm, upper tuffaceous zone, 354 m	1675	san	4	6.81	0.08	48.7	4.4
RG-109	Chamita Fm, upper tuffaceous zone, 354 m	1676	san	9	6.75	0.04	43.7	4.0
RG-117	Chamita Fm, upper tuffaceous zone, 320 m	1677	san	10	6.93	0.05	55.2	6.2
RG-119	Chamita Fm, upper tuffaceous zone, 200 m?	1679	san	7	6.75	0.03	44.8	6.4
RG-120	Chamita Fm, lower tuffaceous zone, 120 m	1683	hbl	9	7.7	0.3	0.08	0.002
RG-42	Tesuque Fm, Skull Ridge member, White Ash #4	2018	san	9	15.42	0.06	14.4	6.1
Peralta Tuff units, Peralta Canyon area								
GSPT-3	tuff of Canada Camada	2351	san	9	6.75	0.09	46.7	2.7
GSPT-4	tuff of Canada Camada	2352	san	9	6.79	0.05	46.4	2.0
GSPT-2	tuff of Colle Canyon	2350	san	9	6.86	0.13	45.7	2.1
GSPT-5	lava correlated to tuff of Peralta Canyon	2353	san	9	6.91	0.06	52.9	1.3
GSPT-1	tuff of West Mesa	2349	san	10	6.96	0.10	53.2	2.6

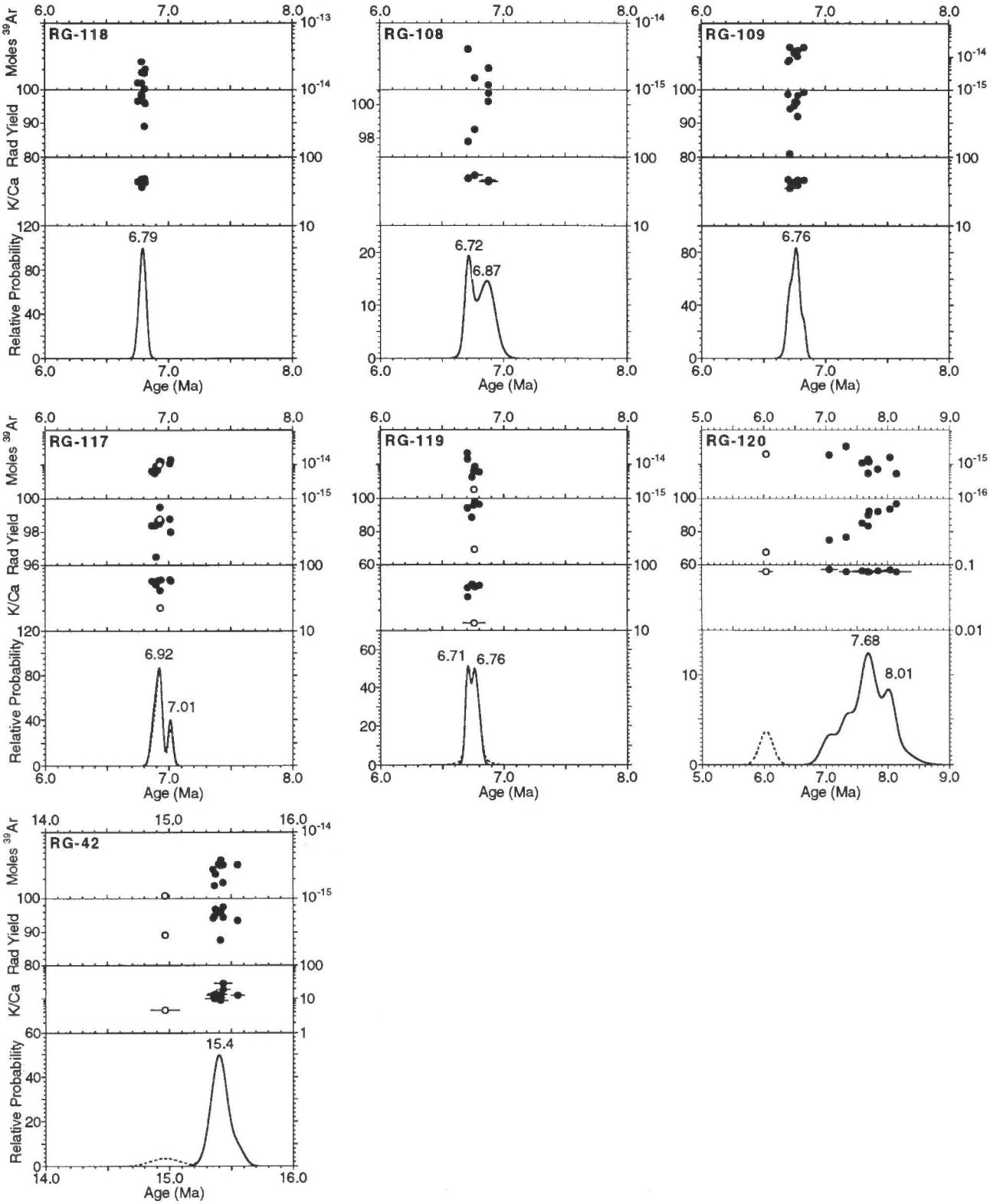


FIGURE 3. Laser-fusion results from ash layers in the Tesuque and Chamita Formations. Values plotted against age for each sample include ideogram curves, moles of ^{39}Ar, radiogenic yield, and K/Ca of individual analyses. The K/Ca vs. age panels show 1s error bars for individual age analyses. The ideogram curves represent the sum of gaussian probability distributions for individual analyses. These curves are similar to histograms, but take into account the uncertainty of each analysis. Dotted and solid lines are, respectively, ideogram curves with and without analyses excluded from mean calculations (shown as open circles). See Table 1 for explanation of sample numbers.

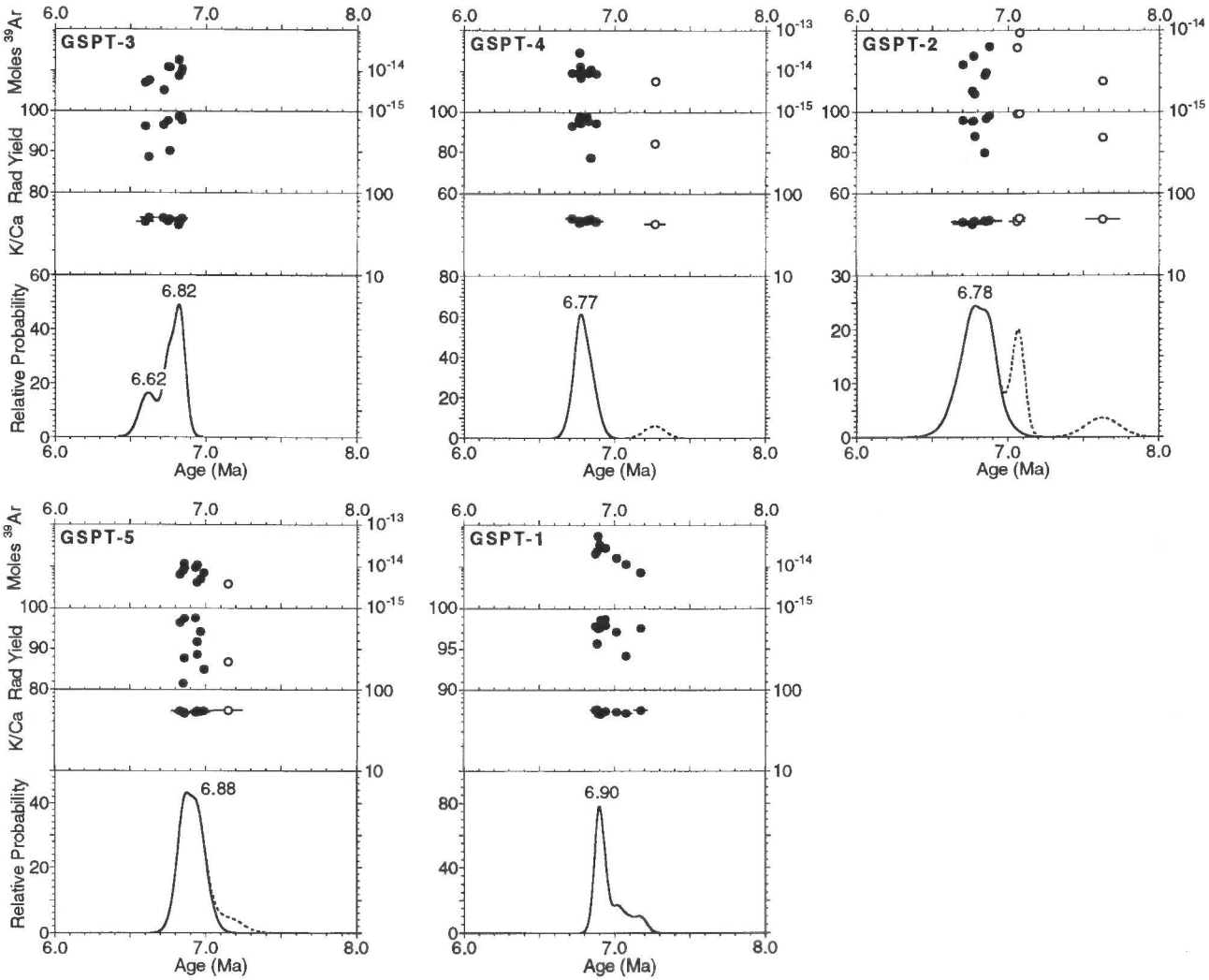


FIGURE 4. Laser-fusion results from Peralta Tuff. See Figure 3 caption for explanation of plots.

samples range from 6.96 to 6.75 Ma; 1s uncertainties in age range from ±0.02 to ±0.13 Ma (±0.3 to ±1.8%), and mean K/Ca values range from 43.7 to 53.2.

Similarly precise ages and high radiogenic yields were obtained from multiple crystal aliquots of fine-grained sanidine from the sample of White Ash # 4 from the Skull Ridge Member (Appendix; Fig. 3). The mean age of nine multiple crystal aliquots from this sample is 15.42 ±0.06 Ma, with a mean K/Ca of 14.4, significantly lower than Chamita Formation sanidines (Table 1). Multiple crystal aliquots of hornblende from tephra near the base of the lower tuffaceous zone of the Chamita Formation yielded individual analyses with lower precision (±1 to ±3%) and lower radiogenic yield (68-97%) than sanidine analyses. Variation among aliquots is also relatively large, giving a mean age of 7.7 ±0.3 Ma (±4 %) (Table 1).

As stated above, separates from 12 of the 24 samples yielded inaccurate ages. These unsuccessfully analysed separates (from samples starred in Fig. 2) include five fine-grained sanidines and seven glass separates from the Pojoaque and Skull Ridge Members. Aliquots of the fine sanidines yielded inconsistent and anomalously old ages (as old as 279 Ma), interpreted as effects of contamination by detrital K-feldspar, probably Precambrian microcline. The glass separates yielded ages that were less anomalous (13-23 Ma), but failed to agree within sampled tephra layers and violated established stratigraphic order. These poor results may reflect potassium loss related to hydration of the glass shards. Age determinations from these 12 fine sanidine and glass separates are not representative of eruption ages of the sampled tephra layers, and were not included in Table 1, Figure 3, or the Appendix.

DISCUSSION

Tesuque Formation

The only precise $^{40}Ar/^{39}Ar$ age determined from the Tesuque Formation is 15.42 ±0.06 Ma for White Ash # 4 in the Skull Ridge Member. This result contradicts fission-track ages of 14.6 and 13.4 Ma previously obtained from zircons in White Ash #2 and #4, respectively (Izett and Naeser, 1986). The 15.42 Ma $^{40}Ar/^{39}Ar$ age, however, agrees closely with the chronology proposed by Barghoorn (1981) and Tedford and Barghoorn (1993), in which White Ash # 4 occurs approximately 20 m below magnetic reversal identified as the base of a short normal polarity interval termed chron C5.Bn.1n and assigned an age of 14.89 Ma by Cande and Kent (1992).

Chamita Formation

$^{40}Ar/^{39}Ar$ results for tephra layers in the Chamita Formation range from 7.67 to 6.75 Ma (Table 1). The oldest dated unit (Fig. 3) is a hornblende-bearing rhyodacitic tephra from the base of the lower tuffaceous zone of Tedford and Barghoorn (1993). Its 7.67 ±0.33 Ma age, although imprecise relative to sanidine analyses, agrees closely with the chronology of Tedford and Barghoorn (1993). In contrast, results from tephras in the upper tuffaceous zone differ significantly from the chronology of Tedford and Barghoorn (1993). Three samples from tephras at the top of this zone (RG-118, RG-108 and RG-109 in Table 1) yielded statistically indistinguishable ages averaging 6.78 ±0.03 Ma. A sample from a tephra at the base of this zone (RG-117 in Table 1) has an age of 6.93 ±0.05 Ma, suggesting that about 0.200 Ma elapsed during the accumulation of the

upper tuffaceous zone. A fifth tephra, separated by faults from the others but thought to be stratigraphically below the 6.93 ±0.05 Ma tephra layer, yielded an anomalously young sanidine age of 6.75 ±0.03 Ma (RG-119 in Table 1). Furthermore, the mean K/Ca of 40.2 for sanidines from this sample also agrees closely with K/Ca values of samples from a layer near the top of the upper tuffaceous zone (Fig. 5). These $^{40}Ar/^{39}Ar$ ages and K/Ca values suggest that the tephra layer may be a fault repeat of stratigraphically higher tephra layers.

The 6.93 to 6.75 Ma range of $^{40}Ar/^{39}Ar$ ages of tephras in the upper tuffaceous zone is significantly older than the 6.6 to 6.0 Ma age for this stratigraphic interval given by Tedford and Barghoorn (1993, fig. 4). $^{40}Ar/^{39}Ar$ results also conflict with fission track zircon ages of 5.3 and 5.6 Ma obtained from the lower and upper tuffaceous zones, respectively, by Manley and Naeser (1977). The $^{40}Ar/^{39}Ar$ results, however, match well with recent revisions of the geomagnetic polarity time scale proposed by Cande and Kent (1992). The chron 3/4 boundary is now assigned an age of 7.245 Ma, and our dates on the upper tuffaceous zone — which is reversely magnetized (MacFadden, 1976, 1977) — would place this tuffaceous interval largely in chron 3Ar. The important late Hemphillian fossils found in the San Juan and Rak quarries are now dated to between 6.93 and 6.75 Ma, significantly older than the 6 Ma indicated by Tedford and Barghoorn (1993).

A comparison the of $^{40}Ar/^{39}Ar$ results from upper tuffaceous zone tephras with results from Peralta Tuff units (Fig. 5) strongly supports a genetic link between the two sequences. If the Chamita Formation sample suspected of being a fault repeat is discounted, then both sequences show a stratigraphically progressive sequence of ages ranging from near 6.95 Ma to 6.75 Ma. This stratigraphic age progression for both sequences is accompanied by a systematic stratigraphic upward decrease in sanidine K/Ca ratios, from values near 52 to values near 45 (Fig. 5, Table 1). These systematic trends in age and geochemistry strongly suggest that the upper tuffaceous zone of the Chamita Formation represents a distal pyroclastic fall facies of the Peralta Tuff, a rhyolite-dome-related pyroclastic sequence erupted from vents in the southeastern Jemez Mountains, 40-50 km southwest of present Chamita Formation outcrops.

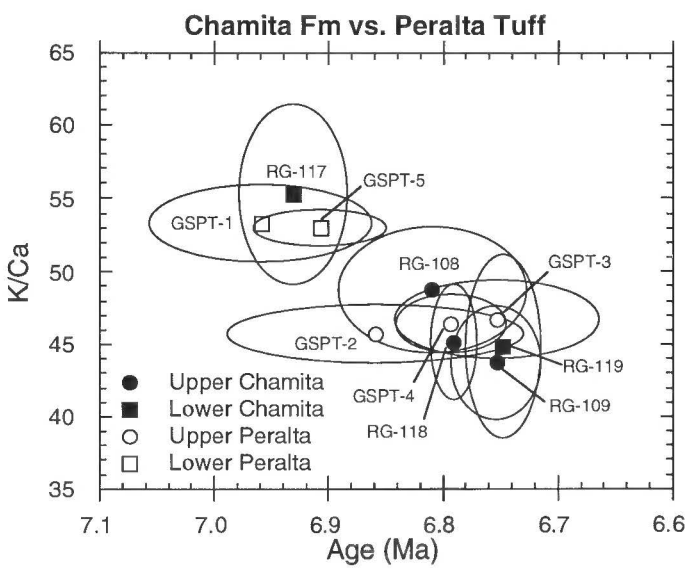


FIGURE 5. Comparison of ages and K/Ca values from the Peralta Tuff and the upper tuffaceous zone of the Chamita Formation. Both units show a similar stratigraphic progression in age and K/Ca values, suggesting that this part of the Chamita Formation is a distal pyroclastic-fall facies of the Peralta Tuff. Sample RG-119 does not fit this progression, probably due to fault repetition in the sampled section. Ellipses represent ±1 s uncertainty in age and K/Ca values.

ACKNOWLEDGMENTS

We are indebted to the Pojoaque and San Juan Pueblos for allowing us to conduct studies on tribal lands, and to Ron Lynch for permission to measure sections across his lease holdings. This study was funded by the National Science Foundation (EAR-9304923). Analyses were performed at the New Mexico Geochronology Research Laboratory, funded in part by the National Science Foundation (EAR-9206438).

REFERENCES

Barghoorn, S., 1981, Magnetic-polarity stratigraphy of the Miocene type Tesuque Formation, Santa Fe Group, in the Española Valley, New Mexico: Geological Society of America Bulletin, v. 92, p. 1027-1041.

Cande, S.C. and Kent, D.V., 1992, A new geomagnetic polarity time scale for the Late Cretaceous and Cenozoic: Journal of Geophysical Research, v. 97, p. 13,917-13,951.

Cather, S.M., 1992, Suggested revisions to the Tertiary tectonic history of north-central New Mexico: New Mexico Geological Society, Guidebook 43, p. 109-122.

Cavazza, W., 1986, Miocene sediment dispersal in the central Española basin, Rio Grande Rift, New Mexico: Sedimentary Geology, v. 51, p. 119-135.

Cavazza, W., 1989, Sedimentation pattern of a rift-filling unit, Tesuque Formation (Miocene), Española basin, Rio Grande Rift, New Mexico: Journal of Sedimentary Petrology, v. 59, p. 287-296.

Galusha, T. and Blick, J. C., 1971, Stratigraphy of the Santa Fe Group, New Mexico: Bulletin of the American Museum of Natural History, v. 144, 127 p.

Ingersoll, R. V., Cavazza, W., Baldridge, W. S. and Shafiqullah, M., 1990, Cenozoic sedimentation and paleotectonics of north-central New Mexico: implications for initiation and evolution of the Rio Grande rift: Geological Society of America Bulletin, v. 102, p. 1288-1296.

Izett, G. A. and Naeser, C. W., 1986, Fission-track ages of air-fall tuffs in Miocene sedimentary rocks of Española basin, Santa Fe County, New Mexico: U. S. Geological Survey, Bulletin 1622, p. 25-29.

MacFadden, B. J., 1976, Magnetic polarity stratigraphy and mammalian biochronology of the Chamita Formation stratotype (Mio-Pliocene) of north-central New Mexico [Ph.D. dissertation]: Columbia University, New York, 114 p.

MacFadden, B. J., 1977, Magnetic polarity stratigraphy of the Chamita Formation stratotype (Mio-Pliocene) of north-central New Mexico: American Journal of Science v. 277, p. 769-800.

Manley, K. and Naeser, C. W., 1977, Fission-track ages for tephra layers in upper Cenozoic rocks, Española Basin, New Mexico: Isochron/West, no. 18, p. 13-14

McIntosh, W. and Harlan, S., 1991, Preliminary $^{40}Ar/^{39}Ar$ age determinations and paleomagnetic results from the Peralta Tuff member, Bearhead Rhyolite, Tent Rocks, Jemez Mountains, New Mexico: New Mexico Bureau of Mines and Mineral Resources, Bulletin 137, p. 101-103.

Rhoads, M. and Smith, G. A., 1995, Contrasting modes of tephra preservation in the Skull Ridge Member of the Tesuque Formation: New Mexico Geological Society, Guidebook 46.

Samson, S. and Alexander, C., 1987, Calibration of the interlaboratory $^{40}Ar/^{39}Ar$ dating standard, MMhb-1: Isotope Geoscience, v. 66, p. 27-34.

Tedford, R. H. and Barghoorn, S. F., 1993, Neogene stratigraphy and mammalian biochronology of the Española Basin, northern New Mexico: New Mexico Museum of Natural History and Science, Bulletin 2, p. 159-168.

APPENDIX—$^{40}Ar/^{39}Ar$ analytical data for Española Basin ashes and Peralta Canyon tuffs.

Run ID#	$^{40}Ar/^{39}Ar$	$^{37}Ar/^{39}Ar$	$^{36}Ar/^{39}Ar$	^{39}K moles	K/Ca	$\%^{40}Ar^*$	Age_1	$\pm Err_2$	SEM_3
RG-118, Chamita ash, 354 m, sanidine, single crystal, J=0.0007971+0.0000002									
1678-09	4.87	1.15E-02	4.97E-04	1.3E-14	44.5	96.6	6.752	0.019	
1678-04	4.79	1.05E-02	1.68E-04	2.7E-14	48.5	98.6	6.782	0.019	
1678-08	4.79	1.08E-02	1.46E-04	1.3E-14	47.2	98.7	6.782	0.020	
1678-03	4.82	1.37E-02	2.65E-04	1.8E-14	37.3	98.0	6.785	0.018	
1678-10	4.92	1.13E-02	5.48E-04	1.8E-14	45.0	96.3	6.806	0.018	
1678-05	5.33	1.04E-02	1.91E-03	1.0E-14	49.2	89.1	6.809	0.025	
1678-02	4.95	1.16E-02	6.25E-04	2.0E-14	43.9	95.9	6.813	0.019	
mean	n=7				45.1 ± 4.0		6.790	0.021	0.008
RG-108, Chamita ash, 354 m, sanidine, single crystal, J=0.0007918+0.0000002									
1675-02	4.81	1.03E-02	2.93E-04	4.1E-15	49.4	97.8	6.713	0.028	
1675-01	4.82	9.34E-03	1.79E-04	1.5E-15	54.6	98.5	6.767	0.060	
1675-08	4.81	1.15E-02	-1.01E-04	1.2E-15	44.3	100.2	6.878	0.072	
1675-05	4.79	1.10E-02	-1.82E-04	2.1E-15	46.6	100.7	6.879	0.052	
mean	n=4				48.7 ± 4.4		6.809	0.083	0.041
RG-109, Chamita ash, 347 m, sanidine, single crystal, J=0.0007881+0.0000002									
1676-07	4.78	1.07E-02	1.47E-04	7.2E-15	47.9	98.7	6.699	0.022	
1676-01	5.84	1.43E-02	3.70E-03	8.2E-15	35.6	81.0	6.711	0.037	
1676-04	5.01	1.14E-02	8.94E-04	2.0E-14	44.6	94.4	6.715	0.020	
1676-03	4.99	1.23E-02	7.40E-04	1.3E-14	41.4	95.3	6.748	0.022	
1676-08	4.93	1.14E-02	5.26E-04	1.5E-14	44.6	96.5	6.753	0.020	
1676-09	4.95	1.15E-02	5.60E-04	1.5E-14	44.5	96.3	6.770	0.021	
1676-06	5.19	1.29E-02	1.35E-03	1.0E-14	39.5	92.0	6.776	0.027	
1676-05	4.85	1.08E-02	2.01E-04	1.6E-14	47.2	98.4	6.777	0.021	
1676-02	4.84	1.09E-02	4.81E-05	1.9E-14	46.9	99.3	6.825	0.018	
mean	n=9				43.6 ± 4.0		6.753	0.040	0.013
RG-117, Chamita ash, 320 m, sanidine, single crystal, J=0.0007912+0.0000002									
1677-02	4.90	8.94E-03	2.06E-04	6.5E-15	57.1	98.4	6.864	0.021	
1677-06	4.91	9.60E-03	1.99E-04	5.7E-15	53.1	98.4	6.889	0.026	
1677-09	5.02	1.01E-02	5.34E-04	9.0E-15	50.3	96.5	6.897	0.019	
1677-07	4.92	8.81E-03	1.57E-04	7.2E-15	57.9	98.7	6.912	0.024	
1677-03	4.94	8.58E-03	1.96E-04	1.3E-14	59.5	98.5	6.925	0.020	
1677-10	*4.92*	*2.27E-02*	*1.37E-04*	*1.0E-14*	*22.5*	*98.8*	*6.929*	*0.019*	
1677-08	4.89	1.24E-02	2.43E-05	1.3E-14	41.1	99.5	6.929	0.017	
1677-01	4.93	8.54E-03	1.51E-04	1.2E-14	59.8	98.7	6.939	0.019	
1677-05	4.98	8.46E-03	1.34E-04	1.1E-14	60.3	98.8	7.009	0.019	
1677-04	5.02	8.86E-03	2.71E-04	1.4E-14	57.6	98.0	7.015	0.020	
mean	n=9				55.2 ± 6.2		6.931	0.051	0.017
RG-119, Chamita ash, 200 m?, sanidine, single crystal, J=0.0008101+0.0000002									
1679-01	4.86	1.15E-02	8.24E-04	2.1E-14	44.2	94.6	6.704	0.018	
1679-03	4.88	1.57E-02	8.97E-04	1.4E-14	32.4	94.2	6.707	0.020	
1679-08	5.22	1.01E-02	1.96E-03	4.2E-15	50.5	88.6	6.741	0.035	
1679-02	4.83	1.06E-02	6.05E-04	6.3E-15	48.1	95.9	6.756	0.024	
1679-10	*6.67*	*3.98E-02*	*6.83E-03*	*1.9E-15*	*12.8*	*69.5*	*6.758*	*0.087*	
1679-05	4.72	1.12E-02	2.22E-04	8.6E-15	45.5	98.2	6.765	0.020	
1679-09	4.82	1.06E-02	4.89E-04	6.0E-15	48.1	96.6	6.800	0.022	
mean	n=6				44.8 ± 6.4		6.745	0.037	0.015
RG-120, Chamita ash, 120 m, hornblende, 10-12 crystals, J=0.0007971+0.0000002									
1683-10B	*6.19*	*6.47E+00*	*8.41E-03*	*2.0E-15*	*0.079*	*67.6*	*6.033*	*0.108*	
1683-09B	6.51	6.06E+00	6.96E-03	1.9E-15	0.084	75.2	7.053	0.126	
1683-07B	6.60	6.49E+00	6.76E-03	3.4E-15	0.079	77.0	7.327	0.101	
1683-08B	6.16	6.30E+00	4.62E-03	1.1E-15	0.081	85.4	7.586	0.140	
1683-03B	5.91	6.43E+00	3.58E-03	1.4E-15	0.079	90.1	7.679	0.097	
1683-06B	6.37	6.57E+00	5.17E-03	5.6E-16	0.078	83.6	7.682	0.232	
1683-02B	5.78	6.58E+00	3.14E-03	1.2E-15	0.078	92.4	7.694	0.157	
1683-05B	5.89	6.31E+00	3.11E-03	7.2E-16	0.081	92.3	7.841	0.171	
1683-01B	5.95	6.12E+00	2.79E-03	1.6E-15	0.083	93.7	8.032	0.088	
1683-04B	5.83	6.54E+00	2.25E-03	5.4E-16	0.078	96.9	8.137	0.234	
mean	n=9				0.080 ± 0.002		7.670	0.333	0.111

APPENDIX—$^{40}Ar/^{39}Ar$ analytical data for Española Basin ashes and Peralta Canyon tuffs.

Run ID#	$^{40}Ar/^{39}Ar$	$^{37}Ar/^{39}Ar$	$^{36}Ar/^{39}Ar$	^{39}K moles	K/Ca	$\%^{40}Ar^*$	Age_1	$\pm Err_2$	SEM_3
RG-42, Skull Ridge, White ash #4, sanidine, 10-40 crystals, J=0.0007369+0.000002									
2018-08	*12.67*	*1.12E-01*	*4.58E-03*	*1.1E-15*	*4.6*	*89.2*	*14.966*	*0.114*	
2018-05	12.32	4.00E-02	2.37E-03	2.8E-15	12.8	94.2	15.354	0.052	
2018-07	12.24	5.22E-02	2.09E-03	1.6E-15	9.8	94.8	15.364	0.072	
2018-03	11.99	3.73E-02	1.21E-03	2.4E-15	13.7	96.9	15.374	0.060	
2018-02	12.10	4.87E-02	1.54E-03	3.4E-15	10.5	96.1	15.399	0.052	
2018-04	13.26	5.76E-02	5.42E-03	3.2E-15	8.9	87.8	15.413	0.059	
2018-01	12.11	3.81E-02	1.51E-03	3.8E-15	13.4	96.2	15.416	0.047	
2018-06	11.95	1.78E-02	9.19E-04	1.7E-15	28.7	97.6	15.434	0.071	
2018-09	12.34	2.72E-02	2.23E-03	3.2E-15	18.8	94.5	15.435	0.053	
2018-10	12.55	3.99E-02	2.66E-03	3.3E-15	12.8	93.6	15.550	0.053	
mean	n=9				14.4 ± 6.1		15.415	0.058	0.019
GSPT-3, tuff of Canada Camada, sanidine, single crystal, J=0.002276766+0.000002									
2351-05	1.67	1.15E-02	1.43E-04	5.1E-15	44.4	96.3	6.599	0.054	
2351-09	1.82	1.02E-02	6.28E-04	5.8E-15	49.8	88.7	6.625	0.055	
2351-04	1.70	1.04E-02	1.24E-04	3.4E-15	49.2	96.6	6.720	0.078	
2351-01	1.68	1.12E-02	6.09E-05	1.3E-14	45.6	97.7	6.750	0.032	
2351-08	1.83	1.07E-02	5.37E-04	1.2E-14	47.8	90.2	6.762	0.036	
2351-02	1.68	1.11E-02	-1.39E-07	7.5E-15	46.1	98.8	6.820	0.043	
2351-03	1.69	1.24E-02	5.49E-06	1.9E-14	41.1	98.7	6.821	0.029	
2351-07	1.69	1.07E-02	3.34E-06	9.3E-15	47.6	98.7	6.836	0.037	
2351-06	1.71	1.05E-02	5.85E-05	1.1E-14	48.5	97.8	6.841	0.033	
mean	n=9				46.7 ± 2.7		6.753	0.090	0.030
GSPT-4, tuff of Canada Camada, sanidine, single crystal, J=0.002284573+0.000002									
2352-03	1.75	1.03E-02	3.41E-04	9.3E-15	49.7	93.1	6.716	0.039	
2352-04	1.71	1.09E-02	1.47E-04	9.3E-15	46.7	96.3	6.761	0.039	
2352-01	1.73	1.15E-02	2.28E-04	3.0E-14	44.2	95.0	6.764	0.028	
2352-06	1.68	1.10E-02	3.90E-05	1.4E-14	46.6	98.1	6.771	0.033	
2352-02	1.74	1.13E-02	2.58E-04	7.1E-15	45.0	94.5	6.774	0.050	
2352-05	1.69	1.08E-02	4.53E-05	9.7E-15	47.3	98.0	6.812	0.036	
2352-10	1.74	1.07E-02	1.98E-04	9.1E-15	47.5	95.5	6.823	0.038	
2352-08	2.15	1.05E-02	1.58E-03	1.2E-14	48.5	77.3	6.840	0.050	
2352-09	1.77	1.12E-02	2.70E-04	8.8E-15	45.7	94.4	6.875	0.043	
2352-07	*2.10*	*1.19E-02*	*1.06E-03*	*5.8E-15*	*42.8*	*84.1*	*7.269*	*0.066*	
mean	n=9				46.4 ± 2.0		6.793	0.049	0.016
GSPT-2, tuff of Colle Canyon, sanidine, single crystal, J=0.002269793+0.000002									
2350-06	1.71	1.15E-02	1.77E-04	3.9E-15	44.2	95.8	6.701	0.071	
2350-07	1.73	1.22E-02	2.01E-04	1.8E-15	41.7	95.4	6.766	0.123	
2350-10	1.73	1.14E-02	1.82E-04	4.9E-15	44.8	95.7	6.772	0.048	
2350-08	1.89	1.12E-02	7.00E-04	1.7E-15	45.4	88.0	6.779	0.142	
2350-05	2.10	1.10E-02	1.38E-03	2.9E-15	46.3	79.7	6.845	0.112	
2350-04	1.73	1.12E-02	1.26E-04	3.1E-15	45.4	96.7	6.854	0.086	
2350-03	1.71	1.09E-02	2.81E-05	6.4E-15	46.7	98.3	6.876	0.045	
2350-02	1.74	1.13E-02	-8.12E-06	6.2E-15	45.2	99.0	7.059	0.048	
2350-01	1.74	1.03E-02	-2.15E-05	9.4E-15	49.3	99.2	7.075	0.037	
2350-9	*2.14*	*1.06E-02*	*8.51E-04*	*2.4E-15*	*48.0*	*87.3*	*7.626*	*0.110*	
mean	n=9				45.7 ± 2.1		6.859	0.130	0.043
GSPT-5, lava correlated to tuff of Peralta Canyon, sanidine, single crystal, J=0.002285407+0.000002									
2353-07	1.72	9.47E-03	1.37E-04	6.5E-15	53.9	96.5	6.828	0.054	
2353-02	2.04	9.77E-03	1.20E-03	8.1E-15	52.2	81.6	6.852	0.056	
2353-03	1.90	9.78E-03	7.12E-04	1.2E-14	52.1	87.8	6.858	0.042	
2353-09	1.71	1.01E-02	6.78E-05	9.3E-15	50.5	97.6	6.859	0.035	
2353-08	1.73	9.76E-03	7.30E-05	9.5E-15	52.3	97.6	6.931	0.040	
2353-06	1.84	9.77E-03	4.42E-04	4.2E-15	52.2	91.8	6.942	0.083	
2353-04	1.90	9.39E-03	6.56E-04	1.1E-14	54.3	88.7	6.943	0.042	
2353-10	1.80	9.57E-03	2.83E-04	5.0E-15	53.3	94.2	6.966	0.053	
2353-01	2.00	9.48E-03	9.42E-04	7.1E-15	53.8	85.0	6.988	0.057	
2353-05	*2.00*	*9.34E-03*	*8.25E-04*	*3.9E-15*	*54.6*	*86.8*	*7.150*	*0.091*	
mean	n=9				52.9 ± 1.3		6.907	0.058	0.019

APPENDIX—$^{40}Ar/^{39}Ar$ analytical data for Española Basin ashes and Peralta Canyon tuffs.

Run ID#	$^{40}Ar/^{39}Ar$	$^{37}Ar/^{39}Ar$	$^{36}Ar/^{39}Ar$	^{39}K moles	K/Ca	$\%^{40}Ar^*$	Age_1	$\pm Err_2$	SEM_3
GSPT-1, tuff of West Mesa, sanidine, single crystal, J=0.002270627+0.000002									
2349-08	1.72	9.06E-03	6.12E-05	2.1E-14	56.3	97.8	6.873	0.030	
2349-07	1.76	8.95E-03	1.89E-04	2.4E-14	57.0	95.7	6.882	0.031	
2349-05	1.73	1.00E-02	7.63E-05	5.6E-14	50.8	97.5	6.891	0.023	
2349-03	1.73	1.02E-02	6.95E-05	3.5E-14	50.0	97.6	6.900	0.025	
2349-04	1.71	1.03E-02	1.01E-05	3.0E-14	49.7	98.6	6.907	0.026	
2349-01	1.72	9.41E-03	6.35E-06	2.9E-14	54.2	98.7	6.937	0.028	
2349-02	1.73	9.45E-03	5.49E-05	2.9E-14	54.0	97.9	6.940	0.029	
2349-10	1.77	9.56E-03	1.05E-04	1.7E-14	53.4	97.1	7.012	0.030	
2349-06	1.84	9.94E-03	2.91E-04	1.2E-14	51.3	94.2	7.075	0.041	
2349-09	1.80	9.17E-03	7.94E-05	7.3E-15	55.6	97.6	7.173	0.042	
mean	n=10				53.2 ± 2.6		6.959	0.098	0.031

Notes: 1. data in italics omitted from calculated means, 2. error is 1 sigma standard deviation,
3. SEM is standard error of the mean.

Analytical parameters:

Espanola Basin tephras - mass discrimination = 1.0066±0.0019, $^{39}Ar_{Ca}/^{37}Ar_{Ca}$=0.0007±0.00005, $^{36}Ar_{Ca}/^{37}Ar_{Ca}$=0.00026±0.0002, $^{38}Ar_K/^{39}Ar_K$=0.0119, $^{40}Ar_K/^{39}Ar_K$=0.019±0.002

Peralta Tuff units - mass discrimination = 1.0044±0.0028, $^{39}Ar_{Ca}/^{37}Ar_{Ca}$=0.0007±0.00005, $^{36}Ar_{Ca}/^{37}Ar_{Ca}$=0.00026±0.0002, $^{38}Ar_K/^{39}Ar_K$=0.0119, $^{40}Ar_K/^{39}Ar_K$=0.021±0.003

All ages relative to Fish Canyon Tuff at 27.84 Ma